


ORIGINAL ARTICLE

A tale of two multi-focal therapies for glioblastoma: An antibody targeting ELTD1 and nitronone-based OKN-007

Michelle Zalles^{1,2} | Nataliya Smith¹ | Debra Saunders¹ | Megan Lerner⁴ |
Kar-Ming Fung^{3,5} | James Battiste^{5,6} | Rheal A. Towner^{1,3} 

¹Advanced Magnetic Resonance Center, Oklahoma Medical Research Foundation, Oklahoma City, Oklahoma, USA

²Oklahoma Center for Neuroscience, University of Oklahoma Health Sciences Center, Oklahoma City, Oklahoma, USA

³Department of Pathology, University of Oklahoma Health Sciences Center, Oklahoma City, Oklahoma, USA

⁴Surgery Research Laboratory, University of Oklahoma Health Sciences Center, Oklahoma City, Oklahoma, USA

⁵Stephenson Cancer Center, University of Oklahoma Health Sciences Center, Oklahoma City, Oklahoma, USA

⁶Department of Neurology, University of Oklahoma Health Sciences Center, Oklahoma City, Oklahoma, USA

Correspondence

Rheal A. Towner, Advanced Magnetic Resonance Center, Oklahoma Medical Research Foundation, 825 NE 13th Street, Oklahoma City, OK 73104, USA.
Email: Rheal-Towner@omrf.org

Funding information

Funding was provided in part by the Oklahoma Medical Research Foundation to R.T.; National Institutes of Health (1S10OD023508-01 to R.T.). Whole slide scanning and image analysis are kindly provided by Peggy and Charles Stephenson Cancer Center at the University of Oklahoma Health Sciences Center, Oklahoma City, OK, an Institutional Development Award (IDeA) from the National Institute of General Medical Sciences (P20 GM103639) and a Cancer Center Supporting Grant Award from the National Cancer Institute (P30 CA225520).

Abstract

Glioblastoma (GBM) is the most common primary malignant brain tumour in adults. Despite a multimodal treatment response, survival for GBM patients remains between 12 and 15 months. Anti-ELTD1 antibody therapy is effective in decreasing tumour volumes and increasing animal survival in an orthotopic GBM xenograft. OKN-007 is a promising chemotherapeutic agent that is effective in various GBM animal models and is currently in two clinical trials. In this study, we sought to compare anti-ELTD1 and OKN-007 therapies, as single agents and combined, against bevacizumab, a commonly used therapeutic agent against GBM, in a human G55 xenograft mouse model. MRI was used to monitor tumour growth, and immunohistochemistry (IHC) was used to assess tumour markers for angiogenesis, cell migration and proliferation in the various treatment groups. OKN and anti-ELTD1 treatments significantly increased animal survival, reduced tumour volumes and normalized the vasculature. Additionally, anti-ELTD1 was also shown to significantly affect other pro-angiogenic factors such as Notch1 and VEGFR2. Unlike bevacizumab, anti-ELTD1 and OKN treatments did not induce a pro-migratory phenotype within the tumours. Anti-ELTD1 treatment was shown to be as effective as OKN therapy. Both OKN and anti-ELTD1 therapies show promise as potential single-agent multi-focal therapies for GBM patients.

KEYWORDS

angiogenesis, blood perfusion rate (BPR), ELTD1, glioblastoma (GBM), monovalent monoclonal antibody (mmAb), MRI, OKN-007, orthotopic G55 xenograft model, tumorigenesis

This is an open access article under the terms of the Creative Commons Attribution License, which permits use, distribution and reproduction in any medium, provided the original work is properly cited.

© 2021 The Authors. *Journal of Cellular and Molecular Medicine* published by Foundation for Cellular and Molecular Medicine and John Wiley & Sons Ltd.

1 | INTRODUCTION

Glioblastomas (GBMs) represent approximately 57% of all gliomas and are the most common primary malignant central nervous system (CNS) tumour.¹ Currently, standard treatment includes surgical resection to remove the bulk tumour, radiotherapy, chemotherapy with temozolomide (TMZ) or bevacizumab, and supportive care.² However, overall survival is poor with a median survival time of 12–15 months.²

The current problem lies with the chemotherapeutic agents. Temozolomide (75 mg/m² daily).

is currently given during radiotherapy followed by another 6 cycles of TMZ.³ TMZ is an alkylating agent that produces DNA lesions, leading to cell death.⁴ Currently, TMZ is the only approved chemotherapeutic agent that has successfully prolonged the overall survival of patients.⁵ However, resistance to TMZ is a key cause of treatment failure. High expression of O⁶-methylguanine-DNA methyl-transferase (MGMT) induces and contributes to TMZ resistance by restoring tumour cell DNA.

Bevacizumab, a humanized monoclonal antibody therapy against the vascular endothelial growth factor (VEGF), is a biologic that is used to combat GBMs. Bevacizumab selectively binds onto circulating VEGF to inhibit its binding onto a receptor (VEGFR) on the surface of endothelial cells.⁶ Although pre-clinical studies showed promise, bevacizumab has not significantly increased overall patient survival in newly diagnosed and recurrent GBM patients.^{6,7} Instead, tumours treated with bevacizumab show increased tumour metastasis and invasion alluding to a pro-migratory phenotype.^{8–10} For example, loss of VEGF signalling has led to a more aggressive tumour phenotype in pre-clinical mouse models.¹¹ Clinically, this pro-migratory phenotype is seen by the development of invasive non-enhancing tumour progression on MRI.¹²

Tumour angiogenesis is greatly upregulated in human high-grade gliomas in order to deliver nutrients and oxygen to the tumour core.¹³ Pro-angiogenic factors such as VEGF and Notch have historically been examined as potential therapies for cancers that are characterized by unregulated angiogenesis. For example, various strategies for inhibiting the VEGF pathway have been investigated. The most common therapy is bevacizumab, which inhibits the binding of VEGF onto its receptors, another is sunitinib which targets the VEGF receptor tyrosine kinase inhibitors (RTKIs).^{9,14} Additionally, four clinical trials (NCT01122901, NCT01119599, NCT01269411 and NCT01189240) were conducted using RO4929097, a Notch signalling pathway inhibitor, against GBMs both as a single agent and in combination with TMZ or bevacizumab.¹⁵ However, from these trials, only one phase 1 trial was completed, while the other three were terminated due to the termination of drug supply from the manufacturer.

ELTD1 (epidermal growth factor, latrophilin and seven transmembrane receptor containing protein 1 on chromosome 1, ADGRL4) has previously been shown to be involved in brain angiogenesis and was shown to be regulated by the VEGF and DLL4/Notch signalling pathways.¹⁶ ELTD1 has higher expression in human high-grade gliomas

when compared to low-grade gliomas.¹⁷ Moreover, targeting ELTD1 with an antibody was found to be effective in a G55 human GBM xenograft mouse model as demonstrated by decreasing tumour volumes, normalizing tumour vasculature and increasing survival.^{18,19} Further optimization of the antibody therapy showed higher binding specificity against the tumour.^{18,19}

OKN-007 (OKN), which was recently found to target the transforming growth factor β 1 (TGF β 1) pathway, is also a small molecule that is effective in crossing the blood-brain barrier.²⁰ From previous pre-clinical studies in U87 and G55 GBM xenografts, and C6, GL261 and F98 high-grade glioma animal models, it was established that OKN is an effective therapy against GBM/high-grade gliomas by inhibiting cell proliferation and tumour necrosis, increasing apoptosis and increasing survival.^{20–24} Recently, it was found that when OKN is combined with TMZ, it increases TMZ sensitivity, thus increasing a significant effect on TMZ-resistant GBM cells.²⁰ OKN is also known to target tumour-associated angiogenesis by targeting and decreasing both VEGFR2a and HIF-1 α protein expression.^{21,25} Currently, OKN is in two GBM clinical trials, (1) phase II open-label OKN combined with TMZ in patients with recurrent GBM and (2) early phase I OKN +TMZ concurrent treatment on patients with GBMs undergoing radiotherapy.

Despite the multimodal therapeutic approach to GBMs, the 5-year relative survival rates are about 5%.² Previous research has demonstrated that single-agent anti-ELTD1 and OKN-007 therapies are effective in GBM pre-clinical models. Therefore, in this study, we aimed to compare the two treatments against each other as well as against bevacizumab, an established GBM treatment in clinics.

2 | MATERIALS AND METHODS

2.1 | Generation of anti-ELDT1 antibodies

Human ELTD1 (Glu20-Leu406) and mouse ELTD1 (Glu20-Leu455) genes were used to create the extracellular domains of human and mouse ELTD1 expression vectors as previously reported.¹⁹ Briefly, the expression vectors were transfected into HEK293F cells (Invitrogen, Carlsbad, CA, USA) and the C_{kappa} fusion proteins were purified from the supernatant using KappaSelect resin (GE Healthcare).

Chickens (white leghorn) were inoculated with a human ELTD1 C_{kappa} fusion protein, where the RNA was obtained from bone marrow, spleen and bursa of the chickens as previously described.¹⁸ Briefly, phage-display library was created from the clones and the positive clones that showed cross-reactivity with human and mouse ELTD1 were selected and enriched determined by Sanger sequencing.

Human or mouse ELTD1 C_k fusion proteins were pipetted onto 96-well microtiter plates (Corning Inc., Corning, NY, USA) in a coating buffer as previously described.¹⁹ 0.1 M NaHCO₃ buffer (pH 8.6) was used to coat the ELTD1 C_k fusion proteins, and then subsequently blocked with 3% (w/v) BSA in phosphate-buffered saline (PBS).

Microtitre plate wells were subsequently incubated and washed as previously reported.¹⁹

2.2 | Glioma model and treatment

Animal studies were conducted with the approval (protocol 17–48) of the Oklahoma Medical Research Foundation Institutional Animal Care Use Committee policies, which follow NIH guidelines. Two-month-old male Athymic Nude-Foxn1nu mice (Harlan Inc., Indianapolis, IN) were implanted with human G55 cells as previously described.^{26,27} The animals were divided into 5 treatment arms: UT, mmAb anti-ELTD1, OKN-007, combined anti-ELTD1 and OKN, and bevacizumab (Genentech). Upon tumour detection (6–7 mm³), the animals were left untreated or were administered with 2 mg/kg of the antibody treatments every 3–4 days (treated M/Th, T/F, W/Sat). OKN-007 (2, 4-disulfophenyl-N-tert-butyl nitron) was administered to the mice in their drinking water at a concentration of 125 mg/kg/day. The amount of OKN-007 consumed by each mouse was determined by weighing water bottles each day. No significant deviation was observed in the volume of liquid uptake of compound in these mice. The average intake of OKN-007 was approximately 140–150 mg/kg/day. All mice were euthanized when tumours reached ≥ 150 mm³.

2.3 | *In vivo* magnetic resonance (MR) techniques

2.3.1 | Morphological imaging

All mice were subjected to MR imaging while under anaesthesia and restrained in a cradle which was inserted into a 30-cm horizontal bore Bruker Biospin magnet (7T, Bruker BioSpin GmbH; Karlsruhe, Germany). The animals were first imaged 10 days post-tumour implantation and then every 3–4 days depending on treatment administration with a BA6 gradient set and mouse coil as previously described.²⁶

2.3.2 | Perfusion imaging

The perfusion imaging method, arterial spin labelling, was used as previously described.²⁸ For perfusion quantification, five region of interests (ROIs) were outlined in the tumour as well as in the contralateral side of the brain as a control. Blood perfusion rates (BPRs) values were determined by subtracting late and early tumour BPRs. This difference was then normalized to BPRs in the contralateral brain region of corresponding animals.

2.4 | Immunohistochemistry and standard staining

Five micron formalin-fixed, paraffin-embedded sections were mounted on HistoBond Plus slides (Statlab Medical Products,

Lewisville, TX). Sections were rehydrated and washed in tris-buffered saline (TBS). Rabbit antibodies were used for CD34 (cat# ab81289, 1:200, Abcam, Cambridge, MA), c-Met (cat# sc-10, 4 μ g/ml, Santa Cruz Biotechnology, Santa Cruz, CA), Caspase-3 (cat# sc-7148, 4 μ g/ml, Santa Cruz Biotechnology, Santa Cruz, CA), Cleaved Caspase-3 (cat# 9661,1:400, Cell Signaling, Danvers, MA), Ki-67 (cat# NB600-1209, 2 μ g/ml, Novus Biologicals, Littleton, CO), CD44v6 (cat# orb13319, 1.7 μ g/ml, biorbyt Ltd, San Francisco CA), TRPM8 (cat# ab3243, 1 μ g/ml, abcam, Cambridge, MA), BMP2 (cat# ab14933, 4 μ g/ml, Cambridge, MA), Notch 1 (cat# ab52627, 11 μ g/ml, abcam, Cambridge, MA), VEGF Receptor 2 (cat# ab2349, 1:100, abcam, Cambridge, MA), L1CAM (cat# ab270455, 1 μ g/ml, abcam, Cambridge, MA). A mouse antibody for anti-Mitochondria (cat# MAB1273, 1:500, Millipore, Temecula, CA) was used to stain mitochondria for human cells. For Immunohistochemistry, slides were processed using Anti-Rabbit IgG ImmPRESS[®] Excel Amplified Polymer kit Peroxidase (cat# MP7601, Vector Labs, Burlingame, CA) or Anti-Mouse IgG ImmPRESS[®] Excel Amplified Polymer kit Peroxidase, (cat# MP-7602, Vector Labs Inc., Burlingame, CA). Antigen retrieval (pH 6 Citrate Antigen Unmasking Solution (cat# H-3300, Vector Labs Inc., Burlingame CA) or a pH 9 tris-based wash (cat# H3301, Vectors Labs, Burlingame, CA) was accomplished via 20 min in a steamer followed by 30 min cooling at room temperature. Sections were then treated with a peroxidase blocking reagent (Bloxall, cat# SP-6000, Vector Laboratories, Inc, Burlingame, CA) to inhibit endogenous peroxidase activity, followed by 2.5% normal horse serum blocking reagent to inhibit nonspecific binding. Appropriate washes were then made in TBS. Antibodies were applied to each section, and following incubation overnight at 4°C in a humidified chamber, sections were washed in TBS. All reagents were applied according to the manufacturer's directions. Slides were incubated with NovaRed[®] (Vector Laboratories, Inc., Burlingame, CA) chromogen for visualization. Counterstaining was carried out with Hematoxylin QS Nuclear Counterstain (Vector Laboratories; Burlingame, CA). Appropriate positive and negative tissue controls were used.

To characterize IHC positivity levels, five regions of interest (ROIs), captured digitally (20 \times) using a Leica-Aperio CS whole slide scanner, were identified in each case. The vessel count algorithm from Leica-Aperio ImageScope was used to count the vessel to determine the MVD. Only areas containing tumour tissue were analysed, excluding areas with necrosis and/or significant artefacts. The number of positive pixels was divided by the total number of pixels (negative and positive) in the analysed area. ROIs were analysed using Leica-Aperio ImageScope and Leica-Aperio Tool Box (pixel count algorithm) (Leica Biosystems, Buffalo Grove, IL).

2.5 | Statistical analysis

Survival curves were analysed using Kaplan-Meier curves. Tumour volumes, perfusion changes and immunohistochemistry protein levels were analysed and compared by one- or two-way ANOVA

with multiple comparisons (Tukey's or Sidak's, respectively). Data were represented as mean \pm SD, and *p*-values of either **p* < 0.05, ***p* < 0.01, ****p* < 0.001, *****p* < 0.0001 were considered statistically significant.

3 | RESULTS

In this study, we aimed to compare OKN-007 therapy and monovalent monoclonal antibody treatments against ELTD1 against the clinically used agent, bevacizumab. Tumour growth was monitored via MRI every 3–4 days, and the animals were either left untreated or treated via tail vein upon tumour detection with either mmAb anti-ELTD1 Ab or bevacizumab (2 mg/kg), or given OKN via the drinking water. Once the tumours reached 150 mm³ (via MRI) mice were sacrificed, and their brains were harvested for histology. The untreated animal and ELTD1 treatment group data were obtained from cumulative studies. As shown in Figure 1A, untreated animals had an average survival of 9 days post-tumour detection. Bevacizumab treatment did not significantly affect percentage of survival and generated an average animal survival of 11 days post-tumour detection. On the other hand, single-agent mmAb anti-ELTD1 and OKN treatments were successful in significantly increasing the overall per cent survival compared to untreated (*****p* < 0.0001 and **0.0025, respectively) and bevacizumab (**p* = 0.0141 and **p* = 0.0277, respectively)-treated animals. Anti-ELTD1 treatment had an average survival of 16 days post-tumour detection meanwhile OKN treatment increased the average survival to 14 days. Combining anti-ELTD1 and OKN treatments significantly increased survival compared to both untreated and bevacizumab-treated animals (***p* = 0.0033 and **p* = 0.0498, respectively). However, there was no additive effect of combining anti-ELTD1 and OKN therapies and therefore no significant difference between the single-agent effect on animal survival compared to the combined therapy.

Animal tumour volumes were assessed based on the average survival of untreated animals. As shown in Figure 1B, untreated animals had an average tumour volume of 130 mm³ at day 9 post-tumour detection. Bevacizumab-treated animals did not significantly decrease the tumour volumes and had an average tumour volume of 94 mm³. Similar to overall survival, anti-ELTD1, OKN and combined groups significantly reduced (****p* = 0.0003, **p* = 0.0416, ***p* = 0.0057, respectively) tumour volumes when compared to untreated animals. Average animal tumour volumes 9 days post-tumour detection can be seen in the representative MR images shown in Figure 1C–G.

To assess microvasculature alterations within the tumour region, we used MRI perfusion to measure the relative change in BPRs. As shown in Figure 2A, normal tissue has an organized vasculature and therefore has a set BPR. However, due to increased angiogenesis, the vasculature becomes chaotic and decreases the perfusion rates within the tissue.²⁹ The untreated animals had a drastic decrease in BPR, shown in the quantitative graph in Figure 2B, which depicts an increase of angiogenesis within the tumour region. Anti-ELTD1 and OKN treatments both normalized tumour vascular perfusion

rates compared to untreated and bevacizumab (anti-ELTD1: UT *****p* < 0.0001, bevacizumab ***p* = 0.0061, OKN: UT *****p* < 0.0001, bevacizumab ***p* = 0.0027). There was significant normalization of the perfusion rates between the combined therapy against both untreated and bevacizumab-treated animals; however, there was no additive effect with the combined therapy (UT *****p* < 0.0001, bevacizumab ***p* = 0.0012). Therefore, we can conclude that anti-ELTD1 and OKN treatments are more effective in normalizing the microvasculature alterations associated with GBMs.

To further examine the effect of each treatment on tumour-associated vasculature, we analysed microvascular density (MVD) of each tumour sample staining for CD34. CD34 is a well known endothelial cell marker for the quantification of angiogenesis.^{30,31} Representative CD34 IHC images are shown in Figure 2C–G. MVD analysis shown in Figure 2H demonstrated that combined treatment significantly decreased MVD within tumour regions compared to untreated, bevacizumab and OKN-treated samples (UT and bevacizumab *****p* < 0.0001, OKN **p* = 0.01). This effect, however, does not seem to be an additive effect from anti-ELTD1 and OKN treatments. Instead, this effect may be mainly attributed to the properties of the anti-ELTD1 as anti-ELTD1 treatment also significantly decreased MVD levels compared to untreated, bevacizumab and OKN treatments (UT and bevacizumab *****p* < 0.0001, OKN ***p* = 0.0055). Although OKN therapy was less effective in decreasing MVD compared to anti-ELTD1, it was still more effective when compared to untreated and bevacizumab therapy (UT *****p* < 0.0001, bevacizumab **p* = 0.011).

The next question then becomes, what is happening with the pro-angiogenic factors, Notch1 and VEGFR2, within the tumour region. Deregulation of the Notch signalling is crucial for tumour development and progression; therefore, we investigated what effects each treatment had on Notch1 positivity levels. The untreated G55 pre-clinical mouse model demonstrates an upregulation of Notch1 staining having an average of 41% Notch1 positivity staining within the tumour region. Bevacizumab treatment did not affect Notch1 staining and also had an average of 48% Notch1 positivity staining, as shown in Figure 3A. As shown in the quantitative graph and representative images in Figure 3A, anti-ELTD1 and combined treatments were successful in significantly decreasing Notch1 positivity staining compared to untreated, bevacizumab and OKN-treated animals (anti-ELTD1: UT, bevacizumab and OKN *****p* < 0.0001; combined: UT ****p* = 0.0008, bevacizumab *****p* < 0.0001, OKN ***p* = 0.0038). There was no significant difference in Notch1 positivity staining when comparing OKN to untreated and bevacizumab-treated animals (see representative images in Figures C–G). The next angiogenic marker in question was VEGFR2. Similar to Notch1, VEGFR2 positivity levels were upregulated, with an average of 61%, in the untreated animals as shown in Figure 3B. As expected, bevacizumab significantly decreased VEGFR2 positivity levels within the tumour region compared to untreated (UT *****p* < 0.0001). Additionally, anti-ELTD1, OKN and combined therapies also significantly decreased VEGFR2 positivity compared to untreated controls (anti-ELTD1 and combined: UT *****p* < 0.0001; OKN: UT ****p* = 0.0002). There

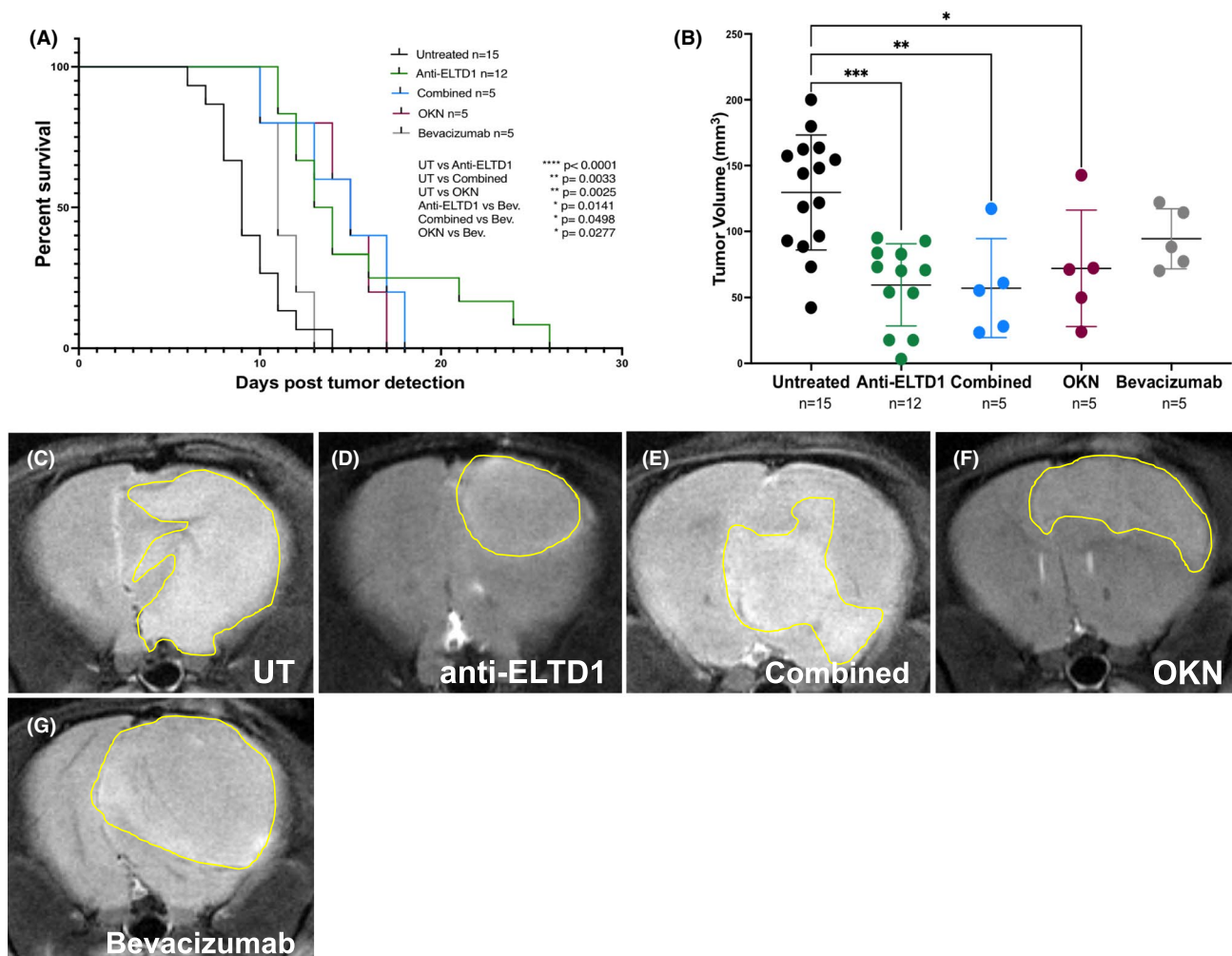


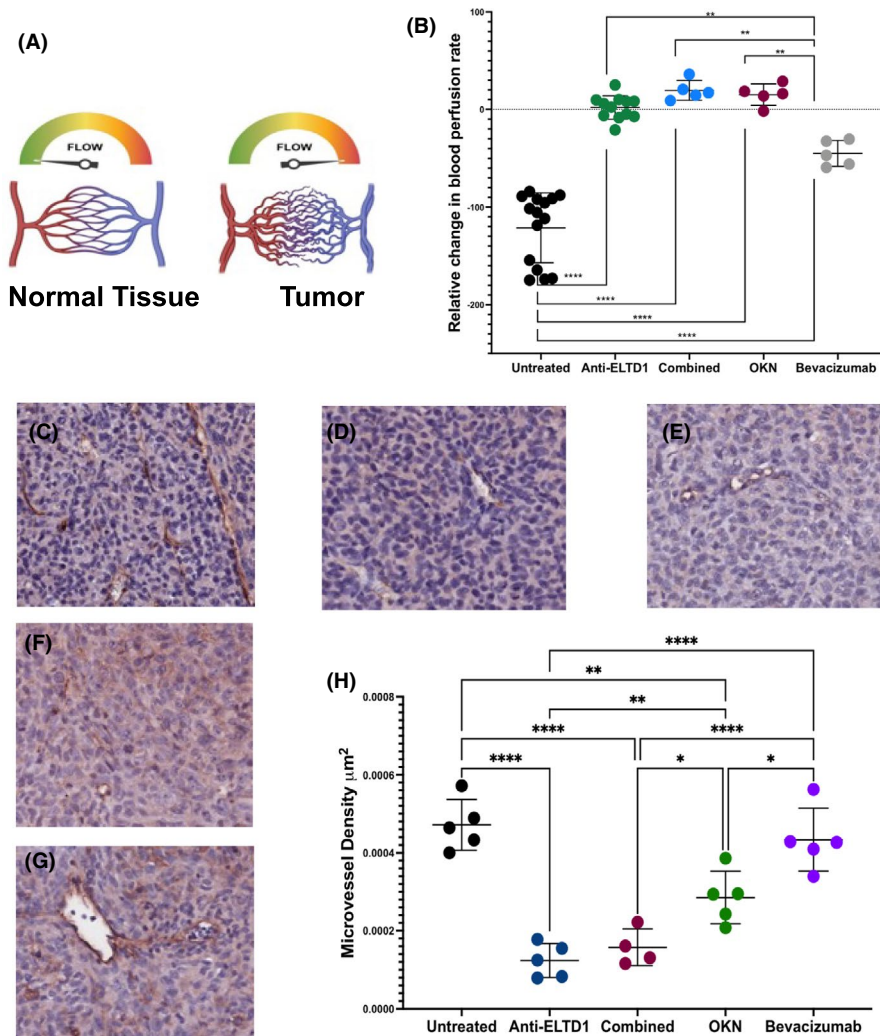
FIGURE 1 Anti-ELTD1 and OKN treatments have similar effects on animal survival and TV. (A) Per cent survival curve for all treatment groups; untreated, anti-ELTD1, OKN, combined anti-ELTD1 and OKN, and bevacizumab treatments. Anti-ELTD1 (**** $p < 0.0001$), OKN (** $p = 0.0033$) and combined (** $p = 0.0025$) groups significantly increased the overall survival post-tumour detection. (B) Tumour volumes of each treatment groups 9 days post-tumour detection. (UT vs Anti-ELTD1 **** $p = 0.0003$, UT vs OKN * $p = 0.0416$, UT vs combined ** $p = 0.0057$) Representative morphological MR images for untreated (C), anti-ELTD1 (D), OKN (E), combined (F), bevacizumab (G) and 9 days post-tumour detection. Tumour boundaries are depicted with yellow lines

was no significant difference between the four treatment groups as shown through the representative images (Figure 3H–L).

We wanted to determine if the effects we were seeing were due to the direct targeting of the human tumour cells (G55 GBM cells). Therefore, we stained the tumour tissue against the human mitochondrial antibody. Figure 4A,B is a representative untreated IHC slice in 1x and 5x, respectively, showing that there is no human mitochondrial antibody staining in the healthy contralateral tissue. The black box and Figure 4B shows the distinct tumour boundaries between the tumour/infiltrating cells and the healthy mouse tissues. Quantification of the untreated animals demonstrates a robust over-expression of human mitochondrial positivity staining within the G55 tumour region (Figure 4C). Anti-ELTD1, OKN and combined therapies, but not bevacizumab, were successful in decreasing the human mitochondrial positivity staining within the tumour region compared to untreated (Figure 4D–H) (anti-ELTD1 vs UT ** $p = 0.0011$; combined vs UT ** $p = 0.0062$; OKN vs UT * $p = 0.0128$).

Bevacizumab studies have demonstrated that therapies that target angiogenesis in GBMs cause an increase of invasiveness by promoting a migratory phenotype to ensure sufficient delivery of oxygen.^{8,14} This, therefore, led us to investigate if our other treatments favoured a pro-migratory phenotype. The transient receptor potential melastatin family member 8 (TRPM8), bone morphogenetic protein 2 (BMP2) and L1CAM are upregulated in GBMs compared to normal brain tissue and are associated with glioma cell proliferation, migration and invasion.^{32–35} To assess tumour cell migration, we first stained the tumour tissue against TRPM8. As shown in Figure 5A, untreated animals had high TRPM8 signalling positivity with an average of 78%. Both bevacizumab and OKN treatments did not have an effect on TRPM8 and instead bevacizumab had an increased average positivity of TRPM8 to 84% while OKN treatment (70%) had a slight decrease from untreated. On the other hand, anti-ELTD1 and combined therapies were all successful in significantly decreasing TRPM8 positivity

FIGURE 2 Anti-ELTD1 and OKN treatments normalize the tumour-associated vasculature within the tumour. (A) Perfusion schematic. The vasculature has a set perfusion rate in normal tissue due to the organized vasculature. The perfusion value decreases as the vasculature within the tumour becomes chaotic. (B) Quantitative analysis of tumour relative blood perfusion rates differences. The perfusion levels were significantly increased with both anti-ELTD1 treatments. Anti-ELTD1, OKN and combined therapies normalized the perfusion levels. (anti-ELTD1: UT **** $p < 0.0001$, bevacizumab ** $p = 0.0061$; OKN: UT **** $p < 0.0001$, bevacizumab ** $p = 0.0027$; combined: UT **** $p < 0.0001$, bevacizumab ** $p = 0.0012$). Representative IHC images (20 \times) for CD34 from untreated (C), anti-ELTD1 (D), combined (E), OKN (F) and bevacizumab (G)-treated animals. Dark red/brown staining in the slides represent vessels in the tumour region. (H) MVD analysis for all of the treatment groups



staining within the tumour region (anti-ELTD1: UT * $p = 0.0132$, bevacizumab ** $p = 0.0045$; combined: UT ** $p = 0.0095$, bevacizumab ** $p = 0.0034$) (Figure 5D–H).

The next migratory marker we investigated was BMP2. Similar to TRPM8, the untreated animals showed an upregulation of BMP2 positivity staining within tumour regions. Again, there was no significant difference between untreated BMP2 levels and bevacizumab or OKN (Figure 5B,I–M). However, we did see a significant decrease between anti-ELTD1 and three of the other groups (untreated, bevacizumab and OKN) (UT *** $p = 0.0004$, bevacizumab ** $p = 0.0029$, OKN **** $p < 0.0001$). Combined anti-ELTD1 and OKN therapy were also successful in decreasing BMP2 levels compared to untreated and OKN treated (UT * $p = 0.0217$, OKN *** $p = 0.0006$).

Unlike the previous two migratory markers, we did not see a robust overexpression of L1CAM in the tumour tissue of untreated animals (32% positivity). Although there was a downward trend of L1CAM positivity with both anti-ELTD1 (11% positivity) and bevacizumab (12% positivity) treatments, there was no significant difference between the two treatments and untreated. Furthermore, both OKN (* $p = 0.0279$) and combined (* $p = 0.0226$) therapies were successful in significantly decreasing L1CAM positivity compared to untreated. These two treatments were also successful in

completely eradicating L1CAM positivity within the tumour region (Figure 5C,N–R).

We then sought to determine if the various treatments had an effect on cellular proliferation within the tumour region. Ki-67 is an established cell proliferation marker that has also been strongly correlated with GBM tumour growth and metastasis.³⁶ As shown in Figure 6A, both untreated (53%) and bevacizumab (51%)-treated animals had high per cent positivity for Ki-67 staining within the tumour region. Anti-ELTD1, OKN and combined therapies were all successful in decreasing Ki-67 positivity compared to both untreated (anti-ELTD1 *** $p = 0.0002$, OKN *** $p = 0.0001$, combined **** $p < 0.0001$) and bevacizumab (anti-ELTD1 *** $p = 0.0006$, OKN *** $p = 0.0003$, combined **** $p < 0.0001$) as shown through the representative images in Figure 6C–G. While there was no significant difference between anti-ELTD1, OKN or combined therapies, combined therapy (11%) seems to have a more significant downward trend when looking at the average Ki-67 positivity within the tumour region when compared against anti-ELTD1 (24%) and OKN (22%) treated.

Aside from tumour angiogenesis, migration and cell proliferation, we wanted to investigate if our therapies had any effect on apoptosis. We stained the tumour tissue against cleaved caspase 3, the activated form of caspase 3, which is used to evaluate the presence

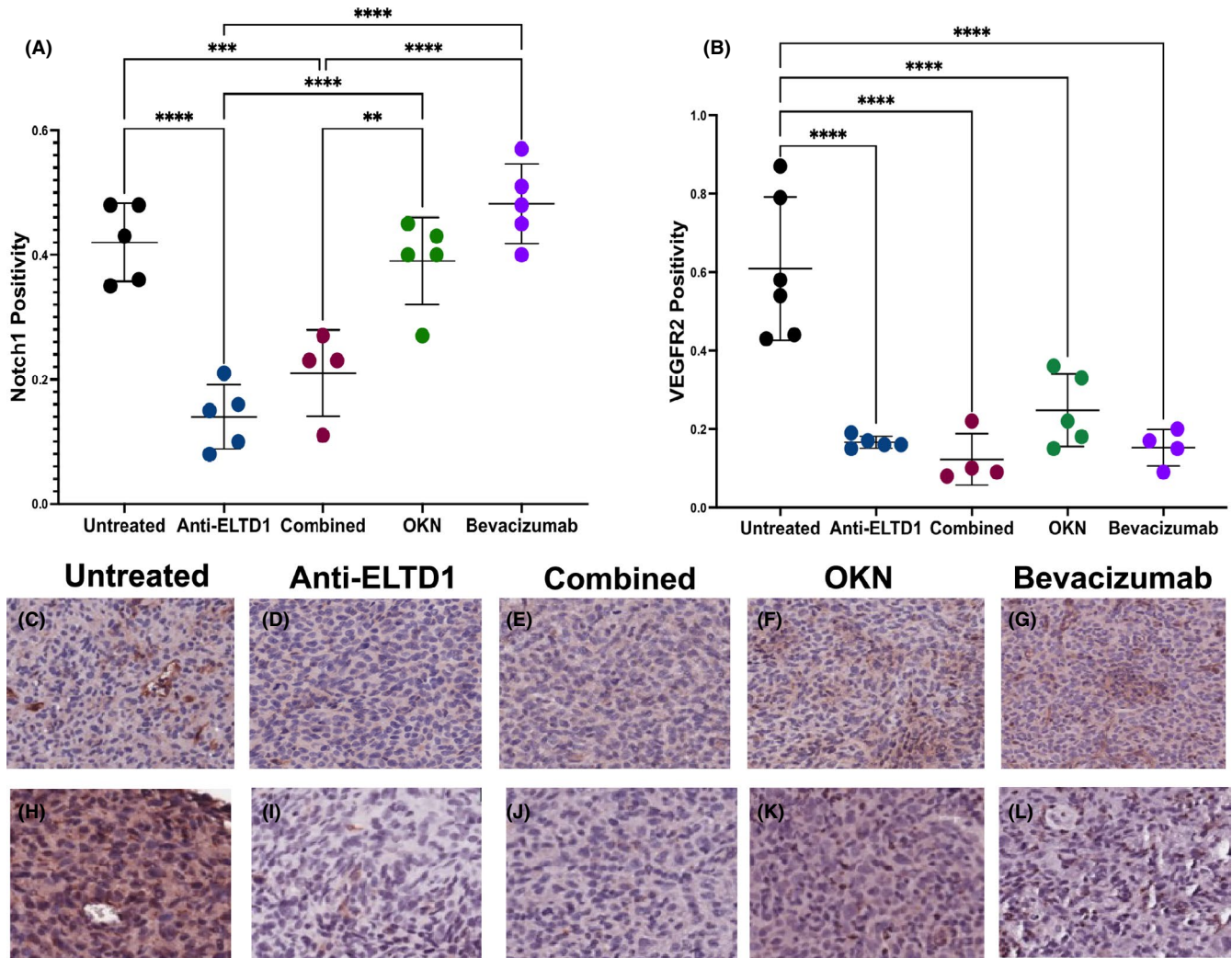


FIGURE 3 Anti-ELTD1 therapy significantly decreased Notch1 and VEGFR2 levels, while OKN treatment only targeted VEGFR2 positivity levels. Quantitative analysis of Notch1 (A) positivity within the tumour region. (anti-ELTD1: UT, bevacicuzumab and OKN **** $p < 0.0001$; combined: UT *** $p = 0.0008$, bevacicuzumab **** $p < 0.0001$, OKN ** $p = 0.0038$) and VEGFR2 (B) staining of the samples. (**** $p < 0.0001$). Representative IHC images (20 \times) for Notch1 from untreated (C), anti-ELTD1 (D), combined (E), OKN (F) and bevacicuzumab (G)-treated animals. Representative images (20 \times) of IHC stained tumours with VEGFR2 of untreated (H), anti-ELTD1 (I), combined (J), OKN (K) and bevacicuzumab (L)

of apoptosis within a given tissue. As shown in Figure 6B, the untreated animals had an average cleaved caspase 3 activity of 54% within the tumour region. All of the treatment groups, Anti-ELTD1 (** $p = 0.0014$), combined (**** $p < 0.0001$), OKN (* $p = 0.0126$) and bevacicuzumab (* $p = 0.0211$), were successful in increasing the apoptotic activity within the tumours. Additionally, as seen through the representative images in Figure 6H–L, combined therapy had a more significant effect in inducing apoptotic activity compared to both bevacicuzumab (* $p = 0.0297$) and OKN (* $p = 0.0473$).

NF- κ B is important for various aspects of cancer biology including resistance to treatment, tumour growth and metastasis.³⁷ G55 untreated and bevacicuzumab-treated animals had robust NF- κ B positivity expression levels in the tumour region. However, as shown in Figure 7, both anti-ELTD1 and OKN therapies were successful in decreasing NF- κ B positivity (anti-ELTD1: UT *** $p = 0.0001$, bevacicuzumab * $p = 0.0408$; OKN: UT * $p = 0.26$). Furthermore, this is

the first marker in which we begin to see an additive effect with the combined therapy (UT, OKN and bevacicuzumab **** $p < 0.0001$, anti-ELTD1 ** $p = 0.0045$). Representative images are shown in Figure 7A–E.

4 | DISCUSSION

This study sought to compare anti-ELTD1 and OKN therapies in an *in vivo* G55 xenograft mouse study. MRI is a powerful tool used by clinicians to monitor tumour progression and clinical effectiveness of prescribed treatment regimens.³⁸ In this study, we used morphological and perfusion MRI to compare anti-ELTD1 and OKN therapies. Both anti-ELTD1 and OKN treatments were significantly better at increasing overall survival when compared to untreated, and there was no significant difference between the two groups. Furthermore,

there was also no significant difference between the two groups with overall tumour volumes.

Typically, the tumour-associated microvasculature alterations associated with tumour angiogenesis is measured by perfusion MRI, which measures a relative change in BPR, and is used to assess the efficacy of anti-angiogenic therapies.³⁹ In GBMs, the tumour-associated vasculature has irregular and leaky vessels that cause the BPR to be lower than the surrounding normal brain.⁴⁰ Once treated with anti-angiogenic therapies, the BPRs within the tumour tend to increase in patients. An explanation to this observation is that there is a decrease of the leaky vessels created by the tumour and instead the remaining vessels mimic normal vessels which results in increased blood perfusion.⁴⁰ In regard to tumour

vascularization, our results showed a drastic decrease in perfusion rates in untreated animals, which is characteristic sign of increased angiogenesis. Although bevacizumab was capable of decreasing this drastic change in perfusion rate, it seems that bevacizumab therapy may not be as effective in normalizing microvasculature within the tumour regions compared to anti-ELTD1 and OKN therapies. Anti-ELTD1 therapy was more successful in decreasing microvessel density levels. Although there was no additive effect with the combined therapy in any of these aspects, MVD levels were significantly decreased compared to untreated, bevacizumab and OKN therapies. Again, our results demonstrate that bevacizumab therapy has no significant effect on the microvascular density levels within the tumour region.

FIGURE 4 Anti-ELTD1 and OKN therapies specifically target human tumour cells. A. Untreated tumour tissue showing human mitochondrial antibody staining (1x). The black box corresponds to (B) and shows that there is no mitochondrial staining in the normal brain tissue (5x). Quantitative analysis of human mitochondrial antibody (C) staining of each group. IHC representative images (20x) of untreated (D), anti-ELTD1 (E), combined (F), OKN (G), bevacizumab (H). (anti-ELTD1 vs UT $**p = 0.0011$; combined vs UT $**p = 0.0062$; OKN vs UT $*p = 0.0128$)

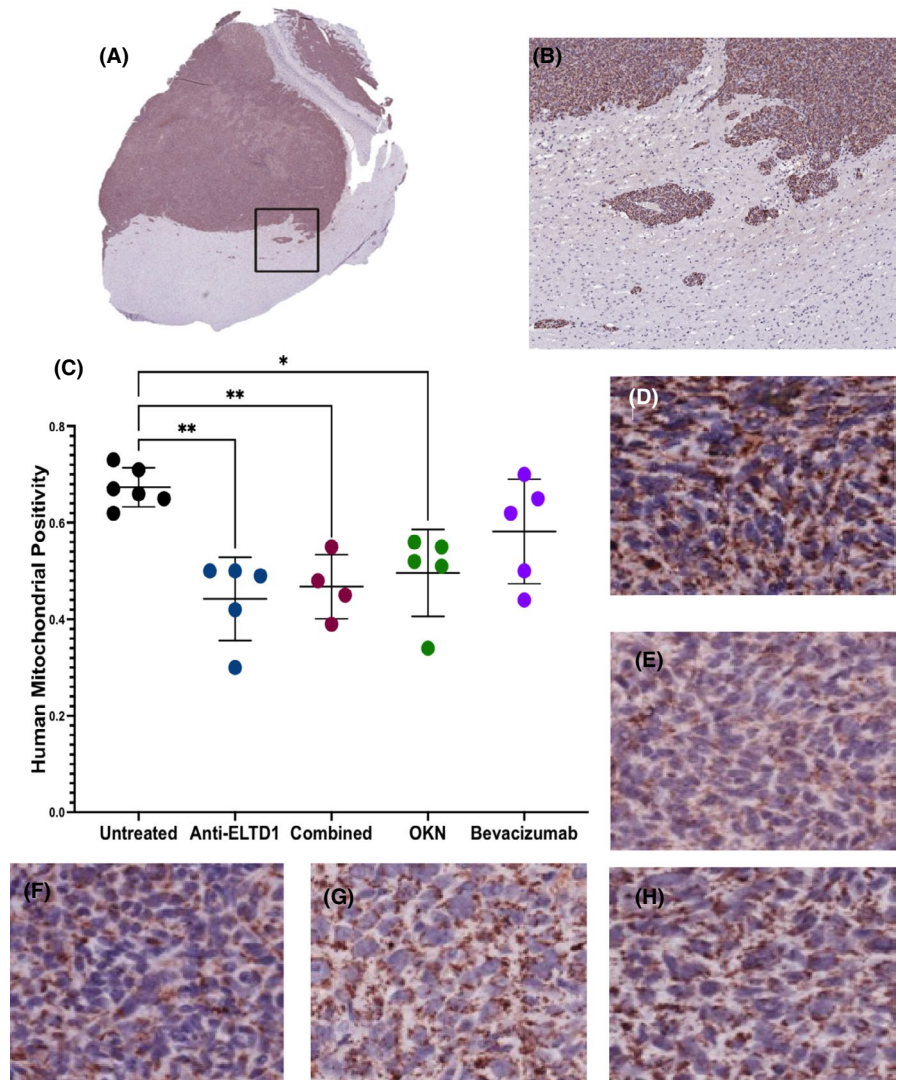
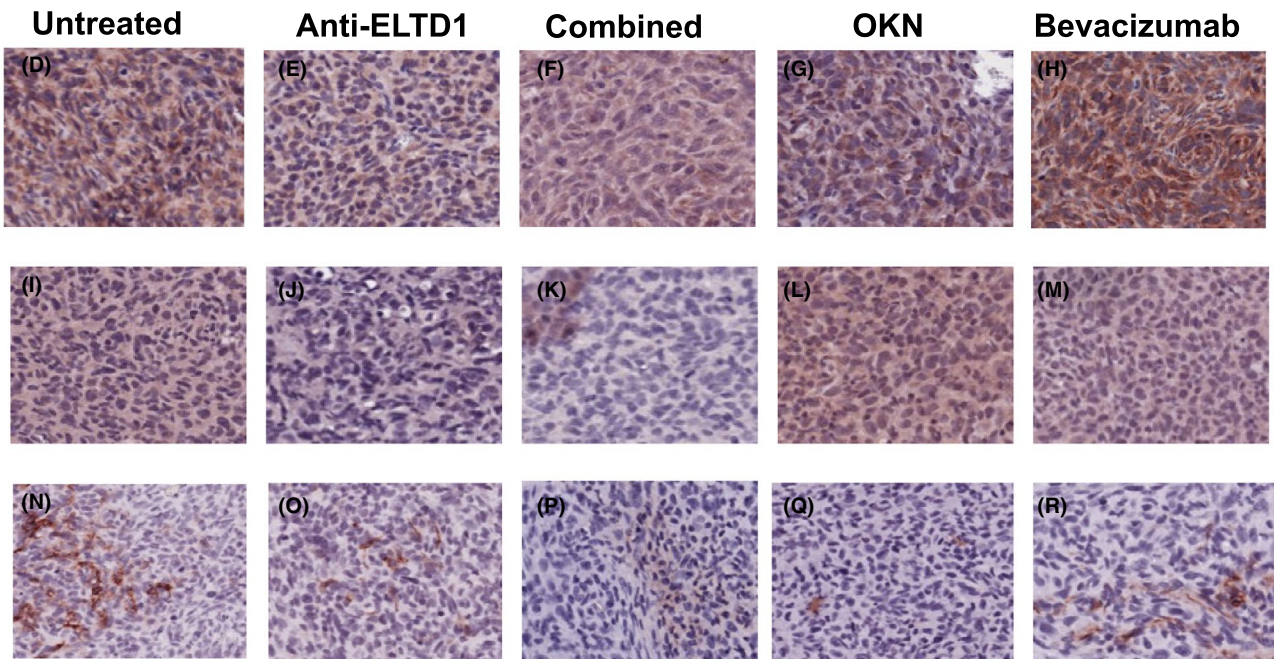
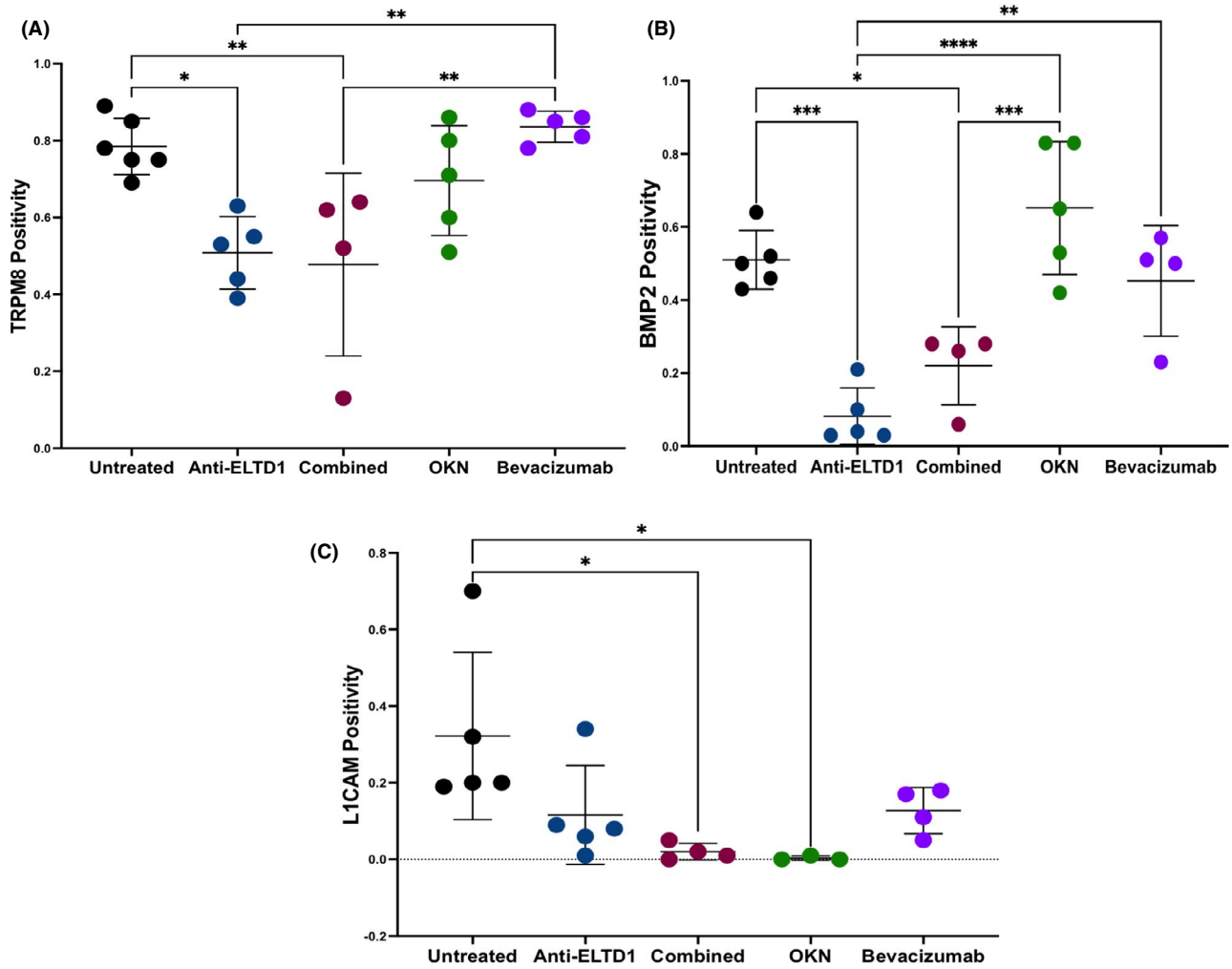


FIGURE 5 Anti-ELTD1 and OKN therapies affect and decrease different migration markers. Quantitative analysis of TRPM8 (A), BMP2 (B) and L1CAM (C) staining of each group. TRPM8 IHC representative images (20x) of untreated (D), anti-ELTD1 (E), combined (F), OKN (G), bevacizumab (H). Representative images (20x) of BMP2 stained tissue samples of untreated (I), anti-ELTD1 (J), combined (K), OKN (L), bevacizumab (M). L1CAM IHC representative images (20x) of untreated (N), anti-ELTD1 (O), combined (P), OKN (Q), bevacizumab (R). TRPM8: anti-ELTD1: UT $*p = 0.0132$, bevacizumab $**p = 0.0045$; combined: UT $**p = 0.0095$, bevacizumab $**p = 0.0034$. BMP2: anti-ELTD1: UT $***p = 0.0004$, bevacizumab $**p = 0.0029$, OKN $****p < 0.0001$). Combined: UT $*p = 0.0217$, OKN $***p = 0.0006$. L1CAM: OKN vs UT $*p = 0.0279$; combined vs UT $*p = 0.0226$



In normal vasculature, ELTD1 expression is regulated by VEGF and Notch/DLL4 pathways.¹⁶ We previously examined the relationship between VEGF and a polyclonal anti-ELTD1 antibody or OKN-007

treatment. In those studies, we demonstrated that ELTD1 and VEGFR2 were co-localized within blood vessels and glioma cells in G55 glioma tumours. The polyclonal anti-ELTD1 treatment significantly reduced

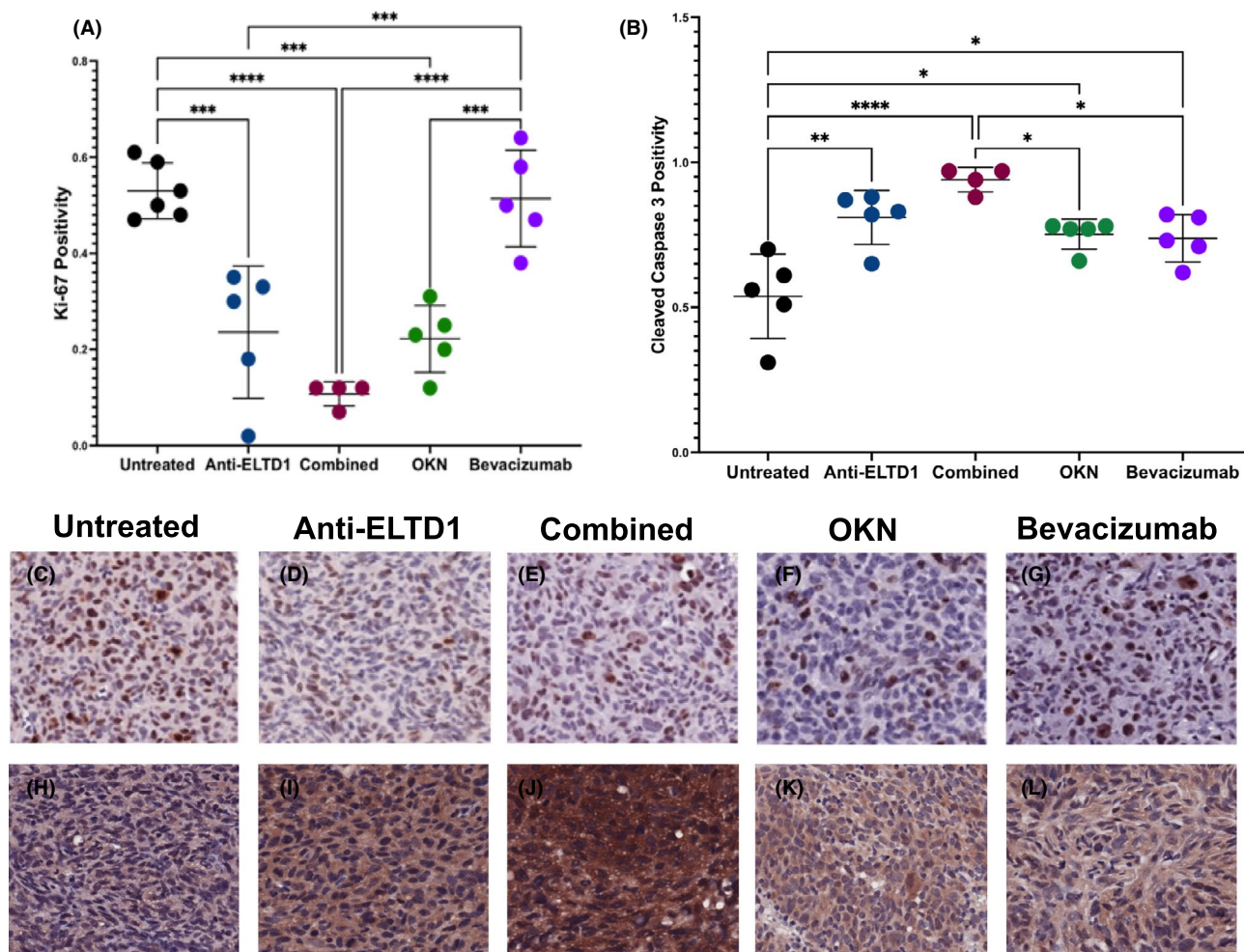


FIGURE 6 Anti-ELTD1 and OKN therapies decrease cellular proliferation and induce apoptosis. Quantitative analysis of Ki-67 (A) and cleaved caspase 3 (B) staining of each group. Ki-67 IHC representative images (20 \times) of untreated (C), anti-ELTD1 (D), combined (E), OKN (F), bevacizumab (G). Untreated vs anti-ELTD1 $***p = 0.0002$, OKN $***p = 0.0001$, combined $****p < 0.0001$ and bevacizumab vs. anti-ELTD1 $***p = 0.0006$, OKN $***p = 0.0003$, combined $****p < 0.0001$. Cleaved caspase 3 IHC representative images (20 \times) of untreated (H), anti-ELTD1 (I), combined (J), OKN (K), bevacizumab (L). Untreated vs. Anti-ELTD1 ($**p = 0.0014$), combined ($****p < 0.0001$), OKN ($*p = 0.0126$) and bevacizumab ($*p = 0.0211$), combined therapy compared to bevacizumab ($*p = 0.0297$) and OKN ($*p = 0.0473$)

the expression of ELTD1 and VEGFR2, but had no significant effect on VEGF.²⁷ In orthotopic rat F98 and human U87 xenograft glioma models, OKN-007 was shown to decrease microvessel density levels as shown through CD31; however, OKN-007 did not alter VEGF levels.⁴¹ In this study, we further demonstrated that in a GBM model, targeting ELTD1 results in decreased expression of both VEGFR2 and Notch1. This further demonstrates that anti-ELTD1 treatment works to decrease several pro-angiogenic factors (although not VEGF) within the tumour region. OKN-007 treatment was also effective in decreasing VEGFR2 expression levels, however, had no effect on Notch1. This further demonstrates that anti-ELTD1 treatment is directly associated with the Notch signalling pathway.

Previous studies have shown that anti-angiogenic therapies, such as bevacizumab, cause GBMs to become progressively invasive and invade normal brain tissue leading to the formation of satellite tumours.⁶ In this study, we sought to determine whether various treatments affected the invasiveness of the tumours by examining the

proliferative rate and the expression of various migratory markers. Bevacizumab treatment had no effect on various migration markers compared to untreated and had a high Ki-67 positivity staining. This suggests that bevacizumab treatment is not effective in decreasing tumour invasiveness.

However, anti-ELTD1 and OKN treatments both significantly decreased Ki-67 positivity suggesting that the tumour is has decreased invasive properties. Additionally, we see that anti-ELTD1 and OKN treatments successfully targeted and decreased migration in our G55 pre-clinical model. Anti-ELTD1 therapy decreased TRPM8 and BMP2, while OKN therapy was successful in decreasing L1CAM positivity levels. This suggests that while anti-ELTD1 and OKN therapies both target migratory pathways, they may have effects on different migration cellular pathways. It was previously shown from microarray analysis that OKN affects tumorigenesis by targeting the TGF- β 1 pathway by downregulating key-associated genes has.²⁰ OKN was shown to downregulate key genes associated with

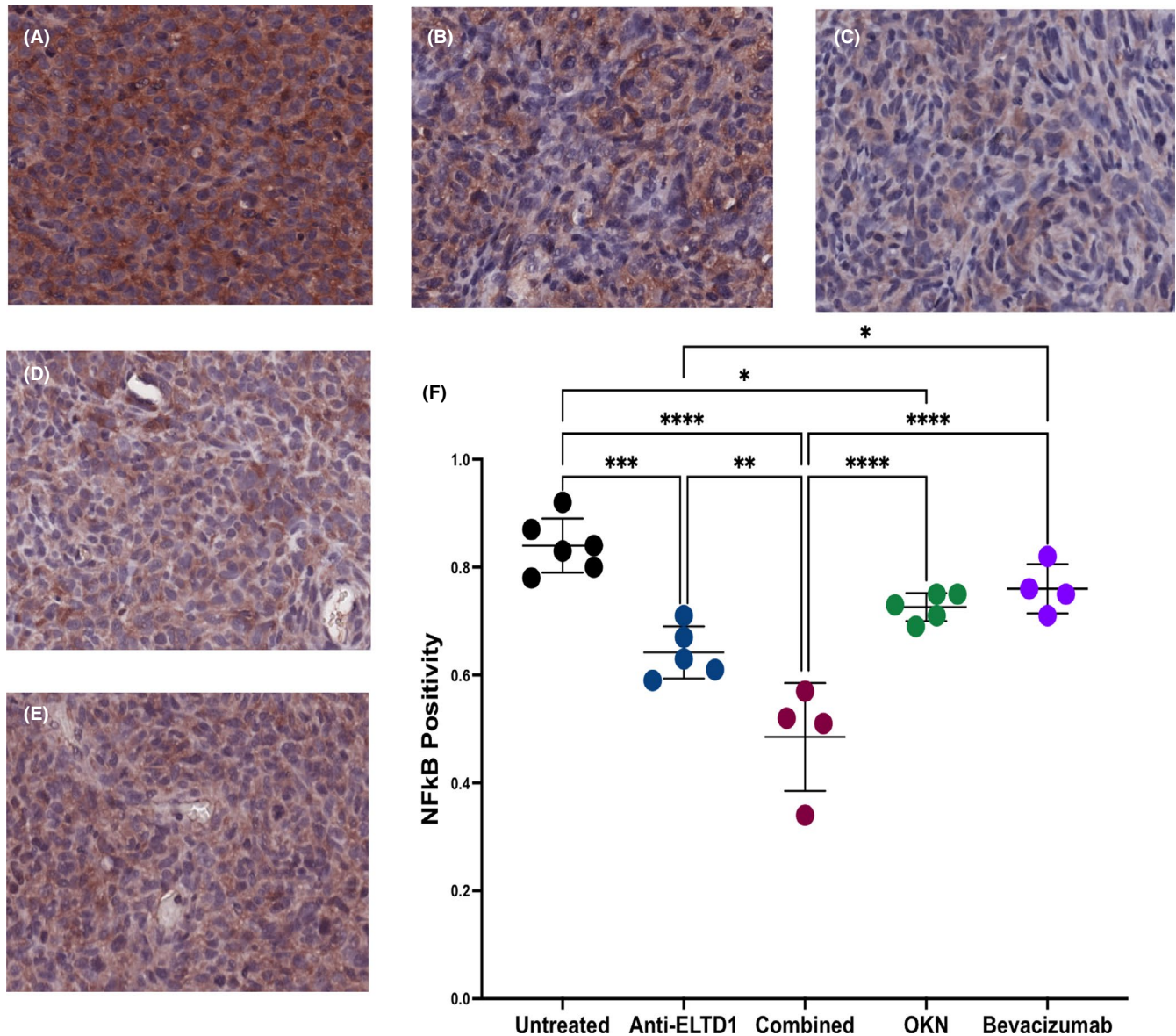


FIGURE 7 Combined anti-ELTD1 and OKN therapies significantly decrease NF- κ B positivity expression levels. IHC representative images (20 \times) of untreated (A), anti-ELTD1 (B), combined (C), OKN (D), bevacizumab (E). Quantitative analysis of NF- κ B (F) staining of each group. Anti-ELTD1: UT *** p = 0.0001, bevacizumab * p = 0.0408; OKN: UT * p = 0.26). Combined: UT, OKN and bevacizumab **** p < 0.0001, anti-ELTD1 ** p = 0.0045

tumorigenesis via microarray analysis and is thought to target the TGF- β 1 pathway.²⁰ Recently, evidence has suggested that the TGF- β and BMP2 pathways may play opposing roles in cancer.⁴² This may explain why OKN-007 did not have a significant effect on BMP2 positivity expression.

Anti-ELTD1 and OKN therapies were both successful in decreasing cellular proliferation and inducing apoptosis within the tumours. Although there was no significant difference within the cellular proliferation marker between the combined treatment compared to the single-agent use of anti-ELTD1 and OKN, there is a downward trend associated with the combined group. Additionally, we do see that the combined treatment is more effective in inducing apoptosis when compared to OKN alone. This therefore provides another advantage for combined therapy. Furthermore, both anti-ELTD1 and OKN

therapies were successful in decreasing NF- κ B positivity levels. The combined therapy showed an additive effect by decreasing NF- κ B positivity expression levels from 84% expression in untreated animals to 49%. This finding suggests that both anti-ELTD1 and OKN treatments target the NF- κ B signalling pathway. NF- κ B is a well known inflammation marker, and both anti-ELTD1 and OKN therapies may have anti-inflammatory effects. OKN has been shown to be an anti-inflammatory agent for age-associated neuroinflammation in a lipopolysaccharide (LPS)-induced encephalopathy rat model.⁴³ Currently, there is little data regarding the relationship between ELTD1 and inflammation, but future studies are needed to investigate this relationship. Further studies are being conducted to determine if Notch1 may be the master regulator of anti-ELTD1 in GBM. Previous RNA-sequencing studies indicate that Notch1 may

be the master regulator of ELTD1. For instance, our data have demonstrated that key genes targeted by anti-ELTD1 antibody therapy, such as c-MET, Ki-67, BMP2 and VEGFR2 are all correlated with Notch1.^{18,19} Anti-ELTD1 therapy has targeted key genes such as c-MET, Ki-67, BMP2 and VEGFR2 which are correlated with Notch1. Therefore, we have reason to believe that Notch1 may be the master regulator of ELTD1.^{18,19}

Further studies will need to be done to confirm the role of Notch 1 in ELTD1 antibody therapy.

5 | CONCLUSION

In preliminary assessments, we saw that anti-ELTD1 and OKN treatments were effective as therapies in a human G55 pre-clinical model. In this paper, we validated those claims by demonstrating that both treatments increased survival, decreased tumour volumes, normalized the tumour-associated vasculature, decreased migratory markers and specifically targeted human tumour cells. Anti-ELTD1 and OKN-007 seem to be similar in most instances; however, combined therapy seems to be more effective than either regarding NF- κ B or better than OKN-007 in inducing apoptosis (cleaved caspase 3).

ACKNOWLEDGEMENTS

This work was made possible by the Oklahoma Medical Research Foundation (RT) and the National Institute of Health (1S10OD023508-01 to RT). The Aperio scanning and image analysis were kindly provided by the Peggy and Charles Stephenson Cancer Center at the University of Oklahoma Health Sciences Center, Oklahoma City, OK, an Institutional Development Award (IDeA) from the National Institute of General Medical Sciences (P20 GM103639) and a Cancer Center Supporting Grant Award from the National Cancer Institute (P30 CA225520). The study was conducted by MZ. The manuscript was written by MZ and was edited by RT, NS and DS. MZ, ML and KMF performed and assisted with the IHC and analysis. RT was the principle investigator.

CONFLICT OF INTEREST

Dr. Towner holds patents for OKN-007 and ELTD1 as a target for GBM. None of other authors have any conflict of interest.

AUTHOR CONTRIBUTIONS

Michelle Zalles: Conceptualization (supporting); data curation (lead); formal analysis (lead); methodology (lead); visualization (lead); writing – original draft (lead). **Nataliya Smith:** Data curation (supporting); investigation (supporting); methodology (supporting); supervision (supporting); writing – review and editing (equal). **Debra Saunders:** Methodology (supporting); supervision (supporting); writing – review and editing (equal). **Megan Lerner:** Methodology (supporting); resources (supporting); writing – review and editing (equal). **Kar-Ming Fung:** Funding acquisition (supporting); methodology (supporting); resources (supporting); writing – review and editing (equal). **James Battiste:** Validation (supporting); writing – review and editing

(equal). **Rheal A. Towner:** Conceptualization (lead); funding acquisition (lead); investigation (lead); project administration (lead); resources (lead); supervision (lead); validation (lead); writing – review and editing (lead).

DATA AVAILABILITY STATEMENT

The data that support the findings of this study are available from the corresponding author upon reasonable request.

ORCID

Rheal A. Towner  <https://orcid.org/0000-0001-7368-8983>

REFERENCES

- Ostrom QT, Gittleman H, Truitt G, Boscia A, Kruchko C, Barnholtz-Sloan JS. CBTRUS statistical report: primary brain and other central nervous system tumors diagnosed in the United States in 2011–2015. *Neuro Oncol.* 2018;20:iv1-iv86.
- Tan AC, Ashley DM, Lopez GY, Malinzak M, Friedman HS, Khasraw M. Management of glioblastoma: state of the art and future directions. *CA Cancer J Clin.* 2020;70:299-312.
- Stupp R, Taillibert S, Kanner A, et al. Effect of tumor-treating fields plus maintenance temozolomide vs maintenance temozolomide alone on survival in patients with glioblastoma: a randomized clinical trial. *JAMA.* 2017;318:2306-2316.
- Kitange GJ, Carlson BL, Schroeder MA, et al. Induction of MGMT expression is associated with temozolomide resistance in glioblastoma xenografts. *Neuro Oncol.* 2009;11:281-291.
- Yi GZ, Huang G, Guo M, et al. Acquired temozolomide resistance in MGMT-deficient glioblastoma cells is associated with regulation of DNA repair by DHC2. *Brain.* 2019;142:2352-2366.
- Li Y, Ali S, Clarke J, Cha S. Bevacizumab in recurrent glioma: patterns of treatment failure and implications. *Brain Tumor Res Treat.* 2017;5:1-9.
- Blumenthal DT, Mendel L, Bokstein F. The optimal regimen of bevacizumab for recurrent glioblastoma: does dose matter? *J Neurooncol.* 2016;127:493-502.
- Narayana A, Gruber D, Kunnakkat S, et al. A clinical trial of bevacizumab, temozolomide, and radiation for newly diagnosed glioblastoma. *J Neurosurg.* 2012;116:341-345.
- Ebos JM, Lee CR, Cruz-Munoz W, Bjarnason GA, Christensen JG, Kerbel RS. Accelerated metastasis after short-term treatment with a potent inhibitor of tumor angiogenesis. *Cancer Cell.* 2009;15:232-239.
- Paez-Ribes M, Allen E, Hudock J, et al. Antiangiogenic therapy elicits malignant progression of tumors to increased local invasion and distant metastasis. *Cancer Cell.* 2009;15:220-231.
- Blouw B, Song H, Tihan T, et al. The hypoxic response of tumors is dependent on their microenvironment. *Cancer Cell.* 2003;4:133-146.
- Iwamoto FM, Abrey LE, Beal K, et al. Patterns of relapse and prognosis after bevacizumab failure in recurrent glioblastoma. *Neurology.* 2009;73:1200-1206.
- Alexander BM, Cloughesy TF. Adult glioblastoma. *J Clin Oncol.* 2017;35:2402-2409.
- Ghiaseddin A, Peters KB. Use of bevacizumab in recurrent glioblastoma. *CNS Oncol.* 2015;4:157-169.
- Gersey Z, Osiason AD, Bloom L, et al. Therapeutic targeting of the notch pathway in glioblastoma multiforme. *World Neurosurg.* 2019;131(252-63):e2.
- Masiero M, Simoes FC, Han HD, et al. A core human primary tumor angiogenesis signature identifies the endothelial orphan receptor ELTD1 as a key regulator of angiogenesis. *Cancer Cell.* 2013;24:229-241.

17. Towner RA, Jensen RL, Colman H, et al. ELTD1, a potential new biomarker for gliomas. *Neurosurgery*. 2013;72:77-90. discussion 1.
18. Zalles M, Smith N, Saunders D, et al. Assessment of an scFv antibody fragment against ELTD1 in a G55 glioblastoma xenograft model. *Transl Oncol*. 2020;13:100737.
19. Zalles M, Smith N, Ziegler J, et al. Optimized monoclonal antibody treatment against ELTD1 for GBM in a G55 xenograft mouse model. *J Cell Mol Med*. 2020;24:1738-1749.
20. Towner RA, Smith N, Saunders D, et al. OKN-007 increases temozolomide (TMZ) sensitivity and suppresses TMZ-resistant glioblastoma (GBM) tumor growth. *Transl Oncol*. 2019;12:320-335.
21. Towner RA, Gillespie DL, Schwager A, et al. Regression of glioma tumor growth in F98 and U87 rat glioma models by the Nitron OKN-007. *Neuro Oncol*. 2013;15:330-340.
22. de Souza PC, Balasubramanian K, Njoku C, et al. OKN-007 decreases tumor necrosis and tumor cell proliferation and increases apoptosis in a preclinical F98 rat glioma model. *J Magn Reson Imaging*. 2015;42:1582-1591.
23. de Souza PC, Smith N, Pody R, et al. OKN-007 decreases VEGFR-2 levels in a preclinical GL261 mouse glioma model. *Am J Nucl Med Mol Imaging*. 2015;5:363-378.
24. Garteiser P, Doblas S, Watanabe Y, et al. Multiparametric assessment of the anti-glioma properties of OKN007 by magnetic resonance imaging. *J Magn Reson Imaging*. 2010;31:796-806.
25. Coutinho de Souza P, Smith N, Atolagbe O, et al. OKN-007 decreases free radical levels in a preclinical F98 rat glioma model. *Free Radic Biol Med*. 2015;87:157-168.
26. Ziegler J, Pody R, Coutinho de Souza P, et al. ELTD1, an effective anti-angiogenic target for gliomas: preclinical assessment in mouse GL261 and human G55 xenograft glioma models. *Neuro Oncol*. 2017;19:175-185.
27. Ziegler J, Zalles M, Smith N, et al. Targeting ELTD1, an angiogenesis marker for glioblastoma (GBM), also affects VEGFR2: molecular-targeted MRI assessment. *Am J Nucl Med Mol Imaging*. 2019;9:93-109.
28. Zhu W, Kato Y, Artemov D. Heterogeneity of tumor vasculature and antiangiogenic intervention: insights from MR angiography and DCE-MRI. *PLoS One*. 2014;9:e86583.
29. van Dijken BRJ, van Laar PJ, Smits M, Dankbaar JW, Enting RH, van der Hoorn A. Perfusion MRI in treatment evaluation of glioblastomas: Clinical relevance of current and future techniques. *J Magn Reson Imaging*. 2019;49:11-22.
30. Aronsson DE, Muhr C. Quantification of sensitivity of endothelial cell markers for the astrocytoma and oligodendroglioma tumours. *Anticancer Res*. 2002;22:343-346.
31. Mei X, Chen YS, Chen FR, Xi SY, Chen ZP. Glioblastoma stem cell differentiation into endothelial cells evidenced through live-cell imaging. *Neuro Oncol*. 2017;19:1109-1118.
32. Zeng J, Wu Y, Zhuang S, et al. Identification of the role of TRPM8 in glioblastoma and its effect on proliferation, apoptosis and invasion of the U251 human glioblastoma cell line. *Oncol Rep*. 2019;42(4):1517-1526.
33. Persano L, Pistollato F, Rampazzo E, et al. BMP2 sensitizes glioblastoma stem-like cells to Temozolomide by affecting HIF-1alpha stability and MGMT expression. *Cell Death Dis*. 2012;3:e412.
34. Wang MH, Zhou XM, Zhang MY, et al. BMP2 promotes proliferation and invasion of nasopharyngeal carcinoma cells via mTORC1 pathway. *Aging*. 2017;9:1326-1340.
35. Kiefel H, Bondong S, Hazin J, et al. L1CAM: a major driver for tumor cell invasion and motility. *Cell Adh Migr*. 2012;6:374-384.
36. Alkhaibary A, Alassiri AH, AlSufiani F, Alharbi MA. Ki-67 labeling index in glioblastoma; does it really matter? *Hematol Oncol Stem Cell Ther*. 2019;12:82-88.
37. Puliappadamba VT, Hatanpaa KJ, Chakraborty S, Habib AA. The role of NF-kappaB in the pathogenesis of glioma. *Mol Cell Oncol*. 2014;1:e963478.
38. Szopa W, Burley TA, Kramer-Marek G, Kaspera W. Diagnostic and therapeutic biomarkers in glioblastoma: current status and future perspectives. *Biomed Res Int*. 2017;2017:8013575.
39. Lee SJ, Kim JH, Kim YM, et al. Perfusion MR imaging in gliomas: comparison with histologic tumor grade. *Korean J Radiol*. 2001;2:1-7.
40. Sorensen AG, Emblem KE, Polaskova P, et al. Increased survival of glioblastoma patients who respond to antiangiogenic therapy with elevated blood perfusion. *Cancer Res*. 2012;72:402-407.
41. Coutinho de Souza P, Mallory S, Smith N, et al. Inhibition of pediatric glioblastoma tumor growth by the anti-cancer agent OKN-007 in orthotopic mouse xenografts. *PLoS One*. 2015;10:e0134276.
42. Ning J, Zhao Y, Ye Y, Yu J. Opposing roles and potential antagonistic mechanism between TGF-beta and BMP pathways: Implications for cancer progression. *EBioMedicine*. 2019;41:702-710.
43. Towner RA, Saunders D, Smith N, et al. Anti-inflammatory agent, OKN-007, reverses long-term neuroinflammatory responses in a rat encephalopathy model as assessed by multi-parametric MRI: implications for aging-associated neuroinflammation. *Geroscience*. 2019;41:483-494.

How to cite this article: Zalles M, Smith N, Saunders D, et al. A tale of two multi-focal therapies for glioblastoma: An antibody targeting ELTD1 and nitron-based OKN-007. *J Cell Mol Med*. 2022;26:570-582. doi:[10.1111/jcmm.17133](https://doi.org/10.1111/jcmm.17133)